Geof. Int. Vol. 23-2, 1984, pp.187-221

AIRBORNE AND GROUND-BASED LIDAR MEASUREMENTS OF THE EL CHICHÓN STRATOSPHERIC AEROSOL FROM 90°N TO 56°S

M. P. McCORMICK*
T. J. SWISSLER**
W. H. FULLER*
W. H. HUNT***
M. T. OSBORN**

RESUMEN

Este trabajo presenta los resultados de cierto número de campañas de observaciones en vuelo mediante el lidar, cubriendo latitudes comprendidas entre los 90°N y los 56°S en el periodo de julio 1982 a enero de 1984. Estos vuelos fueron planeados para determinar las características clave del aerosol estratosférico producido por las erupciones de El Chichón en marzo y abril de 1982. Se discuten asimismo los datos de 10 años de lidar determinados en bases terrestres por la NASA en Langley (37°N). Se describen las tasas de dispersión de fondo, las funciones integradas de dispersión de fondo por aerosol, las densidades columnares de masa y la masa del aerosol estratosférico en relación con la latitud y también con la altitud en los casos adecuados. Se demuestra la existencia inicial de dos regiones generales de capa estratosférica después de la erupción, una arriba de los 20 km de altitud y la otra por debajo de esa altura. El material en suspensión aproximadamente por debajo de los 20 km se desplazó a latitudes más altas, seguido por el material de encima de esa altura, el cual, en su mayor parte, estaba restringido a un cinturón ecuatorial más o menos entre los 10°S y los 30°N, por seis meses aproximadamente. A principios del otoño de 1982, el aumento del material total estratosférico global debido a El Chichón se estimó en 12 megatones. Se cree que el efecto máximo global tuvo lugar entre las misiones de julio y octubre de 1982. Los efectos estratosféricos máximos a los 37°N se experimentaron en enero de 1983. Se vio que la densidad máxima de columna se desplazó hacia el norte con el tiempo. La altitud del pico de material estratosférico se desplazó hacia abajo y la capa se amplió a lo ancho a medida que el material era afectado por el tiempo.

* *Atmospheric Sciences Division, National Aeronautics and Space Administration, Langley Research Center, Hampton, VA 23665*

** *Systems and Applied Sciences Corporation, Hampton, VA 23666*

*** *Wyle Laboratories, Hampton, VA 23666*

ABSTRACT

This paper presents the results of a number of airborne lidar campaigns, covering latitudes from 90°N to 56°S over the period July 1982 to January 1984.. These flights were designed to determine key characteristics of the stratospheric aerosol produced from March-April 1982 eruptions of El Chichón. Also discussed is the 10-year ground based lidar data set at NASA Langley (37°). Backscatter ratios, integrated aerosol backscatter functions, column mass densities, and mass of the stratospheric aerosol versus latitude and, where appropriate, altitude are described. Two general stratospheric-layer regions are shown to exist initially after the eruption, one above 20 km and one below 20 km. The material below about 20 km moved to higher latitudes, followed by the material above 20 km which for the most part, was constrained to an equatorial belt between about 10°S and 30°N for approximately 6 months. In the early fall of 1982, the total global stratospheric increase due to El Chichón was estimated to be 12 megatonnes. The maximum global impact is thought to have occurred between the July and October 1982 missions. Maximum stratospheric effects at 37°N were experienced in January 1983. The maximum column density was seen to move north in time. The altitude of the peak of stratospheric material moved downward and the layer broadened in width as the material aged.

INTRODUCTION

The March 28, April 3, and April 4, 1982, eruptions of the volcano El Chichón in Mexico (17.33°N, 93.2°W) probably produced the largest enhancement in stratospheric aerosols experienced in the last 70 years. Certainly, it was the largest measured by active and satellite-borne remote sensors. The early values of lidar backscatter ratio and optical depth were record setting with the most massive part of the stratospheric cloud centered at 26-27 km in low latitudes.

The impact of this cloud on satellite remote sensors and the earth's radiation became evident very rapidly. For example, the NOAA Advanced Very High Resolution Radiometer (AVHRR) began experiencing artifacts or offsets in their sea surface temperature (SST) retrievals compared to ground truthings (Strong, 1984) due to the absorption of infrared radiation by the El Chichón-produced sulfuric acid stratospheric layer. Similarly, instruments aboard the Solar Mesospheric Explorer (SME) satellite received emission from the layer in infrared channels designed to measure water vapor and ozone, and received scattering from the layer in spectrometer channels from 0.3 to 2.4 μm designed to measure NO_2 and other species (Barth *et al.*, 1983). Although producing artifacts in SST, water vapor, ozone and NO_2 measurements, the data from both these satellites have been successfully used to study the formation and dynamics of the El Chichón-produced cloud. The radiative effects of the volcanic cloud on the atmosphere were also immediately realized with a significant stratospheric warming at the layer location (Labitzke *et al.*, 1983; Quiroz, 1984; and Labitzke and Naujokat, 1984).

The magnitude of this eruption is such that it should provide the scientific community with a real test for the various models that predict stratospheric transport and dispersion, aerosol radiative effects, and the effects of aerosols on chemistry and the measurements made by remote sensors. Model calculations have already

predicted significant effects (Robock, 1984; McCracken and Luther, 1984; Vupputuri and Blanchet, 1984; Pollack and Ackerman, 1983).

The importance of this eruption prompted NASA to organize a series of airborne lidar measurement campaigns covering the latitudes from 90°N to 56°S. These were supported with optical depth, diffuse and total radiation, SO_2 and O_3 remote measurements from aboard the participating aircraft. In addition, supporting *in situ* measurements were made from coordinated balloon and high-altitude aircraft platforms. This paper describes the results of lidar measurements made during these flights and the long-term, ground-based lidar measurements made at NASA, Langley Research Center (37°N, 76°W).

OBSERVATIONS

Ground-based measurements at Langley, 37°N

The lidar data presented in this paper will be in three forms: the lidar backscatter ratio, the lidar aerosol backscatter ratio, and the integrated aerosol backscatter function (or just integrated backscatter). The lidar backscatter ratio is defined as

$$R(z) = 1 + f_A(z)/f_M(z)$$

where f_A is the aerosol backscatter function ($m^{-1}\,ster^{-1}$) and f_M is the molecular backscatter function, both at altitude z. The aerosol backscatter ratio is simply R-1. The integrated aerosol backscatter function is defined as

$$\int_{h_T}^{h_M} [R(z) - 1]\, f_M(z)\, dz$$

where h_T and h_M are the heights of the tropopause and maximum height (usually 28-30 km), respectively.

Figure 1 is a long-term lidar data set taken from Langley. Plotted is the integral of the aerosol backscatter function versus time, integrated from the tropopause upward to about 30 km which, at this latitude, is high enough to include most of the aerosols in the stratosphere. All data in this paper are for the ruby laser wavelength of 0.6943 μm. The vertical arrows on the abscissa indicate the times of major volcanic eruptions. A listing of eruptions for the period 1974 to 1982, thought to be energetic enough to place material into the stratosphere, is given in Table 1. Note in Figure 1 the increased volcanic activity of the past 4 years. The first major eruption during this period was that of Mount St. Helens, May 18, 1980. This was followed by the low latitude eruption of Ulawun which occurred as the stratospheric material from Mount St. Helens was decaying. Subsequent eruptions continued this upward trend in stratospheric loading with the largest perturbation being caused by

Table 1

Major volcanic eruptions 1974 - 1982

Source	Location		Date	
Fuego	14.5°N	90.9°W	14 October	1974
Augustine	59.4°N	153.4°W	22 January	1976
Sierra Negra	0.8°S	91.2°W	13 November	1979
Mt St. Helens	46.2°N	122.2°W	18 May	1980
Ulawun	5°S	151.3°E	7 October	1980
Alaid	50.8°N	155.5°E	27 April	1981
Pagan	18.1°N	145.8°E	15 May	1981
Mystery cloud	Tropical source		1 - 20 January	1982
El Chichón	17.3°N	93.2°W	28 March	1982
			3 - 4 April	1982

the 1982 eruptions of El Chichón. From the low values of 1979 to the peak reached in January 1983, a 100-fold increase in stratospheric integrated backscatter was experienced. Although indicative of overall northern hemispheric volcanic perturbations, Figure 1 shows the record at 37°N, and as such, should not be extrapolated to global values. Subsequent airborne lidar data will give a better, albeit not total, picture of the global impact. Global mass calculations using fixed site data are only fortuitously representative of global values.

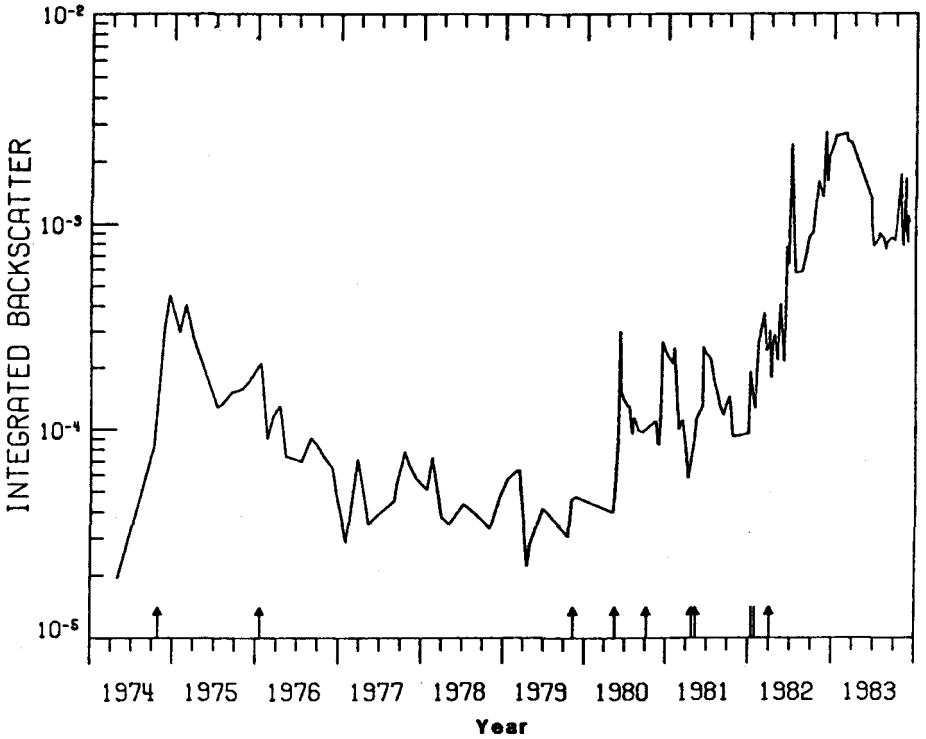

Fig. 1. Integrated aerosol backscattering function from the tropopause through 30 km at $\lambda = 0.6943$ μm versus time for ground-based lidar data taken at 37°N, 76°W. The arrows indicate the date of major volcanic eruptions (see Table 1).

The spiked increased and rapid decay such as that recorded after the Mount St. Helens eruption are usually indicative of a source near the latitude of the lidar, especially if there is subsequent decay in the integrated backscatter. Low latitude eruption material usually shows up in the mid-latitude integral after some delay, increases to a maximum, and then decays. For example, the October 1980 eruption of Ulawun was first detected in the lidar measurements in December 1980. The shape of the vertical profile also gives an idea of whether a layer is from a recent eruption, with sharp boundaries on thin layers being more representative of a fresh layer. It also helps to separate a more recent eruption from a previous one.

As the initial El Chichón cloud spread zonally, circling the globe in about 3 weeks driven by summertime easterlies (Matson and Robock, 1984), the first lidar station to make measurements was at Mauna Loa, "downwind" of El Chichón. The cloud spread meridionally with material below about 19 km moving slowly toward the poles. However, the material above 19 km, which contained most of the original mass, was confined to the northern tropics. The first indication at Langley of this new perturbation was measured on April 29, 1982, as the lower altitude material moved north. On July 1, 1982, a piece of material from the upper layer appeared over Langley centered at 25 km with a peak scattering ratio of 45. The bulk of the upper cloud, however, remained at low latitudes at this time, as will become evident later in this paper. The peak in integrated backscatter at 37°N was reached in January 1983. The following decay period shows a slow summertime decrease and then some transient enhancements in October through December, caused by Arctic air mass transports over Langley. These events broaden the layer in altitude by advecting in lower-latitude, aerosol-laden material from high-latitude. The result is sometimes a doubling of the column content.

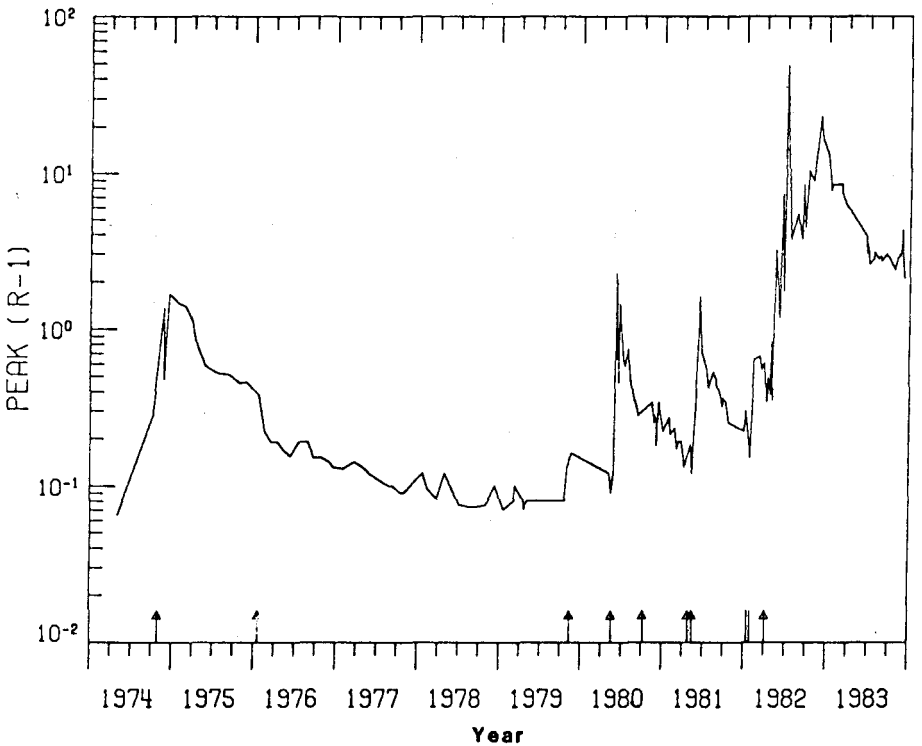

Fig. 2. Peak aerosol backscatter ratio versus time (as in Figure 1).

Figure 2 gives another perspective of the time history at a fixed site. Here, the aerosol peak backscatter ratio value (R - 1) is plotted versus time. A 400- to 600-fold increase is seen from the background values in 1978-79 to the peak values of 1982. In this case, however, the low latitude Ulawun eruption and the Arctic outbreaks do not show up as definitively. The Ulawun material spent a considerable amount of time in the Tropics as a zonal band and then moved northward over our station with lower peak values similar to the aged Mount St. Helens values at that time. Similarly, the Arctic air intrusions in the fall of 1983 were well aged and, therefore, very broad in altitude extent with peak values similar to the material existing over Langley at that time at a higher altitude.

Figure 3 plots the altitude and width of the peak backscatter layer. Typically, the layer peak is higher in non-volcanic periods. The perturbations of 1980-1981 show lower peak altitudes, but El Chichón placed material at an unusually high altitude. At Langley, as mentioned above, the layer was centered at 25 km for a short period in 1982. It slowly lowered to 15-20 km where the 1980-1981 eruptions and the Fuego and Augustine clouds of 1974-1976 were located. In general, the width of the layer is broad when there is very little volcanic activity and quite variable and narrow for fresh volcanic conditions. The width broadens as the layer ages.

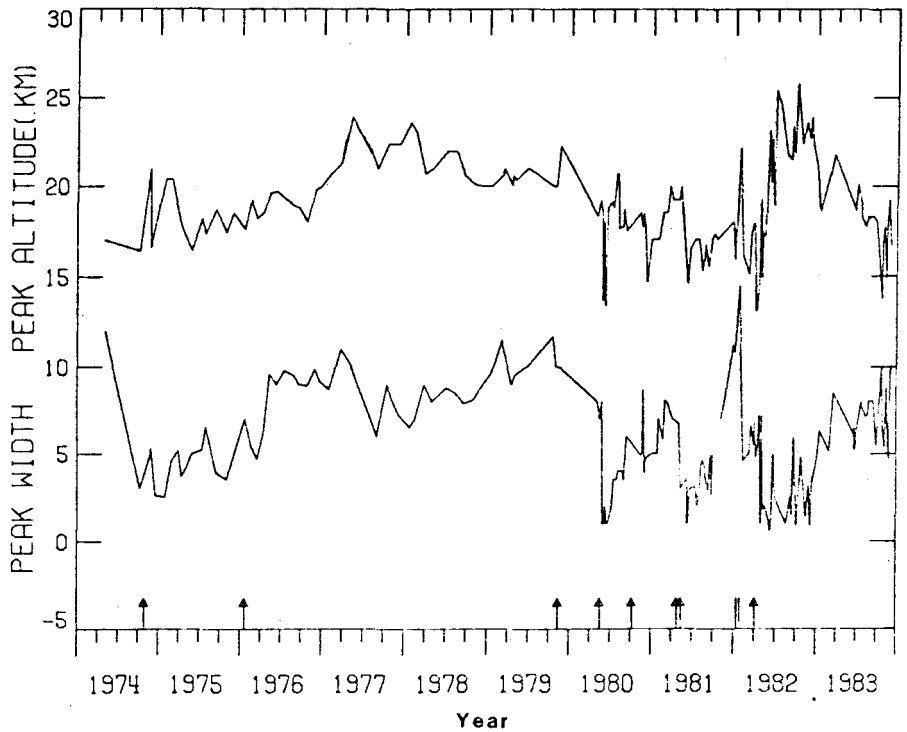

Fig. 3. The altitude of the peak aerosol backscatter ratio (top) and the width of the peak layer (bottom) versus time (as in Figure 1).

Figure 4 gives examples of lidar backscatter ratio versus altitude for measurements made at Langley after the El Chichón eruption. The changes are obvious with both peak ratio and altitude decreasing in time. The July 1 and October 27, 1982, measurements are representative of an enhancement of the low-altitude upper layer at that time. The January 3 profile shows the peak integrated conditions; the layer then decreased in scattering ratio and in peak height.

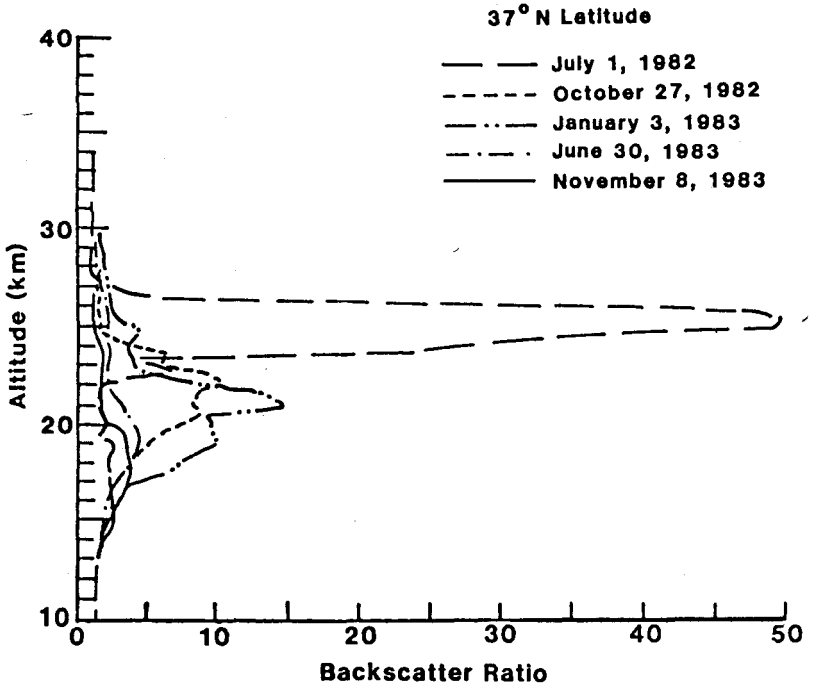

Fig. 4. Lidar profiles of backscatter ratio (R) at $\lambda = 0.6943$ μm versus altitude for ground-based data taken at 37°N, 76°W.

AIRBORNE CAMPAIGNS

Introduction

Presently, NASA has the SAM II and SAGE satellites in orbit specifically designed to measure stratospheric aerosols. SAM II is the Stratospheric Aerosol Measurement-II experiment, and SAGE is the Stratospheric Aerosol and Gas Experiment. Both utilize the technique of solar occultation to produce vertical profiles of aerosol extinction at 1 μm wavelength during each spacecraft sunrise and sunset (McCormick *et al.*, 1979). SAM II was launched in October 1978 aboard the spacecraft Nimbus 7 in a high noon sun-synchronous orbit. This constrains SAM II's measurements to the earth's two polar regions. SAGE, on the other hand, is aboard the

AEM-2 spacecraft in a highly precessing orbit which provided sunrise and sunset measurements between about 70°N and 70°S. Whereas SAM II is still operational, monitoring stratospheric aerosols at high latitudes, the AEM-2 spacecraft batteries failed in November 1981 before the El Chichón eruption, thus terminating SAGE measurements. Prior to this time, however, SAGE provided much data on the eruptions between 1979 and 1981 (Newell and Deepak, 1982; McCormick, 1983).

Because SAGE was not available to provide mid- and low-latitude data, and because of the previously mentioned importance of the effects of the El Chichón eruption, NASA organized and sponsored a number of airborne campaigns to provide the latitudinal distribution of aerosol characterization needed for model calculations. Figure 5 shows the ground tracks for five coordinated lidar missions using the Langley lidar. The airborne lidar is, of course, much smaller than the Langley ground-based system but uses a similar computer-controlled data acquisition system and ruby laser ($\lambda = 0.6943\ \mu m$).

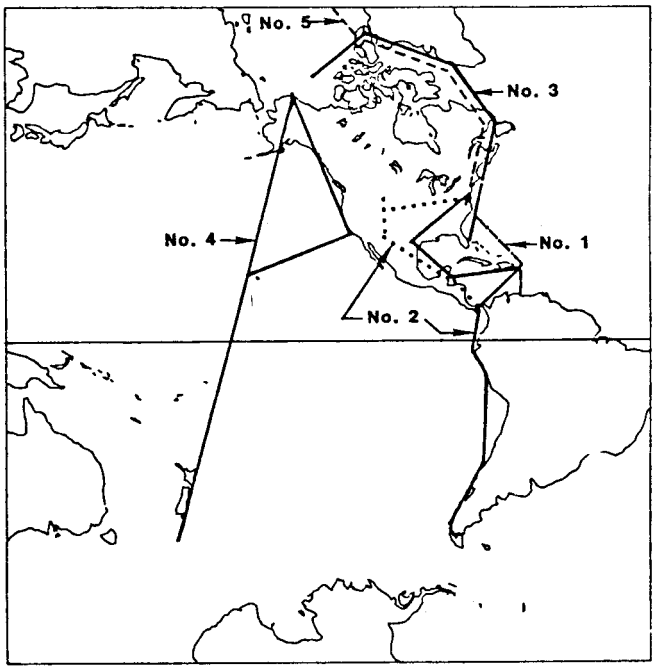

Fig. 5. Ground tracks for the NASA Langley airborne lidar measurement campaigns.

In December 1982 another dedicated NASA El Chichón mission was flown, but without a lidar. It covered from 6°S to 55°N and had on board instruments to measure optical depth, diffuse and total solar radiation, SO_2, and O_3. The NASA Electra was used for all but the May 1983 flight shown in Figure 5; the NASA CV-990 was used for the December 1982 and May 1983 flights. In addition, NASA

supported a number of high altitude U-2 flights with *in situ* samplers aboard to further characterize the time evolution of the layers.

Some of the results from these missions have been published prior to this issue. For example, some of the results from the July 1982 campaign were published in Geophysical Research Letters (GRL) Vol. 10, No. 1, January 1983, by Labitzke *et al.*; some of the results from the October-November 1982 campaign in four papers in GRL (Vol. 10, No. 4, May 1983, by Hofmann and Rosen, and Vol. 10, No. 9, September 1983, by McCormick and Swissler *et al.*; and Spinhirne) and one in Science (Vol. 222, No.4621, October 1983, by Hofmann and Rosen); and finally, some of the results of the December 1982 campaign were published in a special issue of GRL (Vol. 10, No. 11, November 1983). This issue contains a number of additional papers that present airborne or supporting data from these missions.

July 1982 campaign

The first flight shown in Figure 5 was exploratory in nature and occurred in July 1982 from NASA Wallops Flight Center (38°N) to the Caribbean to determine something about the cloud's latitudinal and vertical distributions. It covered latitudes from upstate New York (42°N) to off the northern coast of Venezuela (12°N) Figure 6 shows some example profiles from this campaign. Note that below about

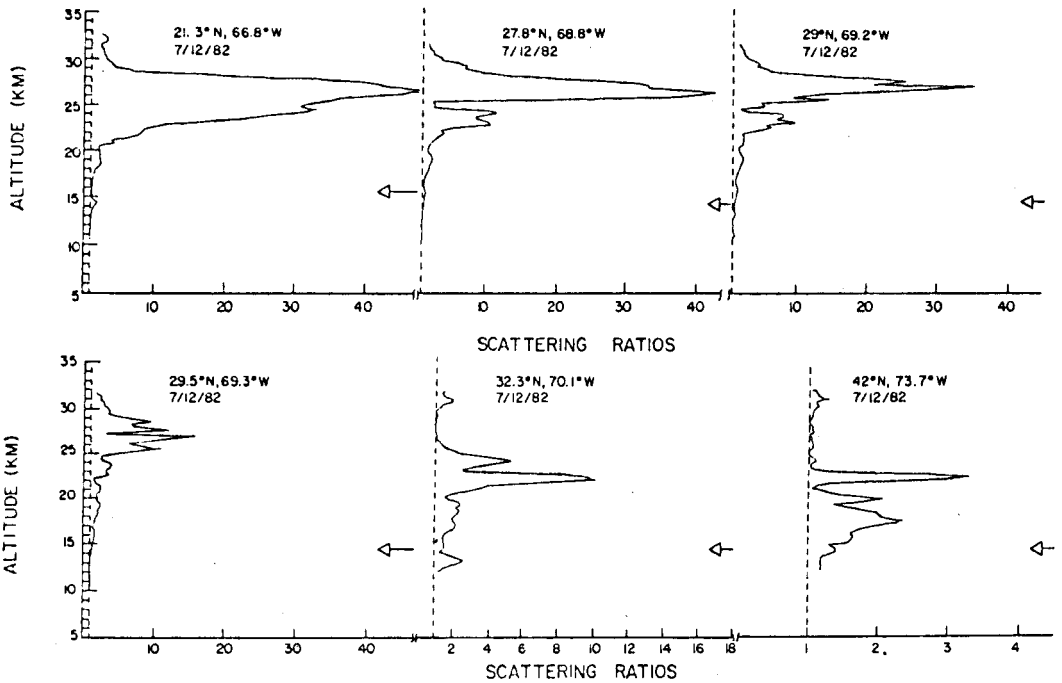

Fig. 6. Airborne lidar profiles of backscatter ratio at $\lambda = 0.6943$ μm versus altitude taken during the July 1982 campaign.

20 km, scattering ratios of 2 to 3 were measured over these latitudes, but above 20 km a distinct ledge was found over the latitudes of Florida at about 30°N. Scattering ratios of about 40 were recorded south of 30°N throughout the Caribbean. The tropopause heights are indicated in Figure 6 by the horizontal arrows on the right side of each profile; the latitudes and measurement dates (in this case July 12, 1982) are shown in each panel.

Figure 7 shows the results of the lidar measurements in the form of contours of aerosol backscatter ratio as a function of height and latitude. The northbound and southbound legs are shown separately and the latitude of El Chichón is indicated by the vertical arrow on the southbound abscissa. The sharp boundary near 30°N is evident, especially for the northbound flight. The limit of the highest ratios (peaked at about 27 km) is at about 28°N for both legs of the campaign. The stratospheric integrated backscatter for these profiles is shown in Figure 8. The ledge near 30°N is very evident. This quantity can be converted to column density or optical depth by knowing the physical/optical characteristics of the layer versus altitude, and will be described with each flight.

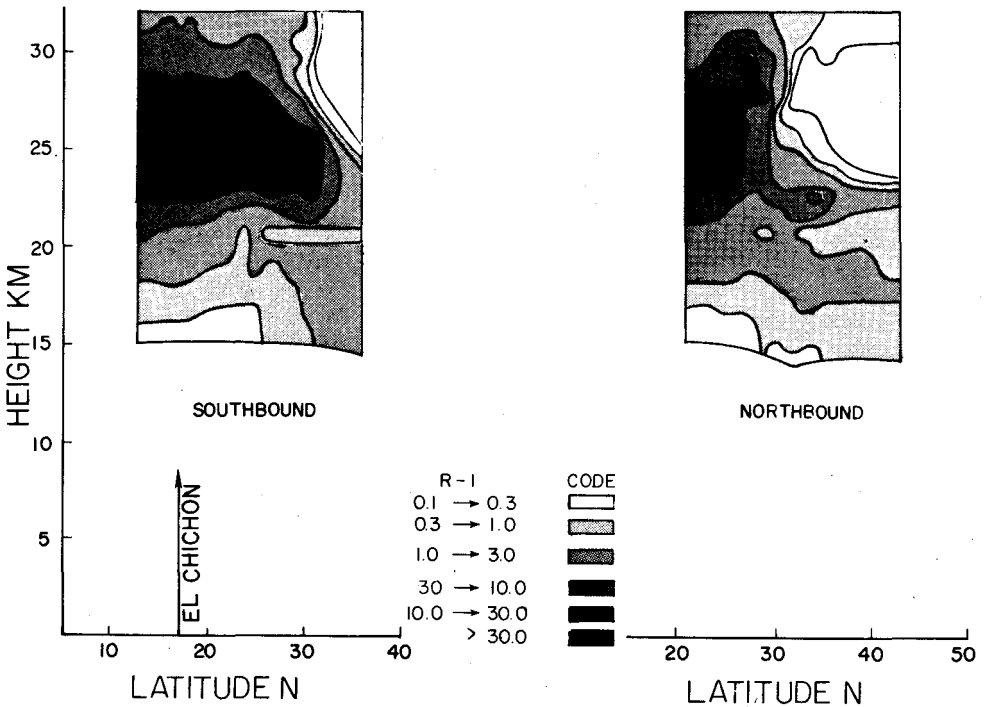

Fig. 7. Contours of aerosol backscatter ratio (R-1) at $\lambda = 0.6943$ μm versus altitude and latitude for the July 9-12, 1982 flight campaign.

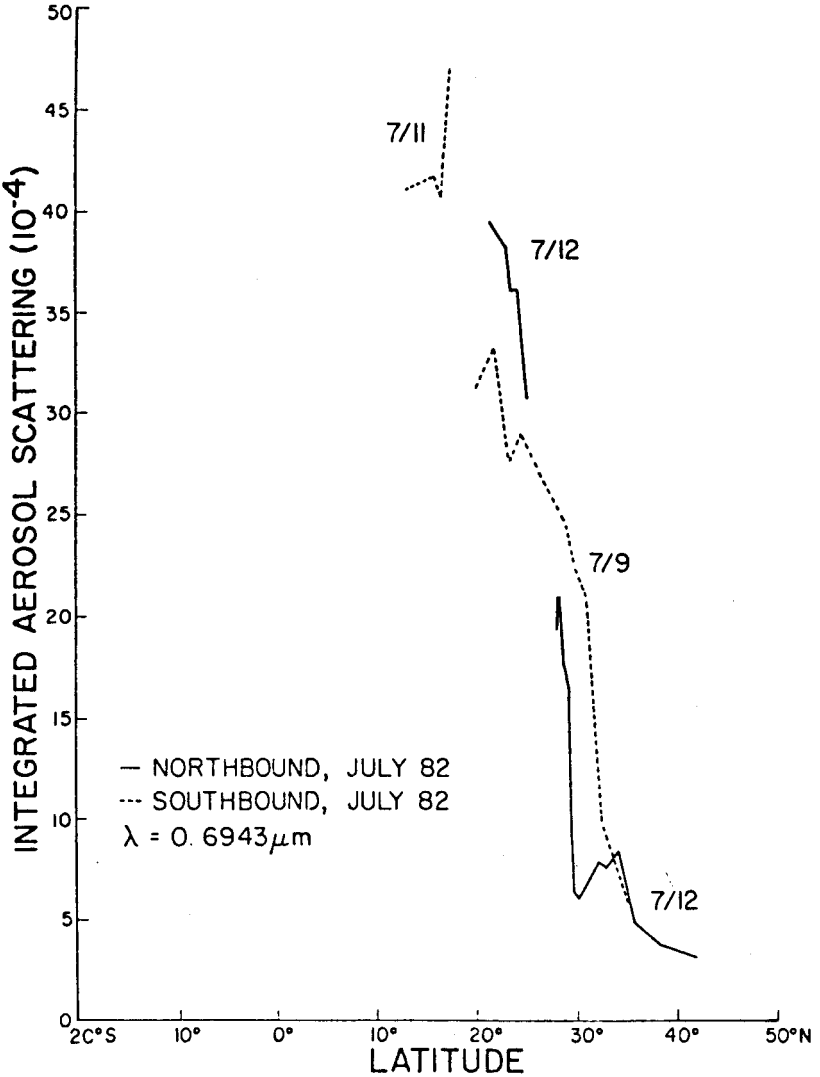

Fig. 8. Integrated aerosol scattering function at $\lambda = 0.6943$ μm from the tropopause through the stratospheric layer versus latitude for the southbound and northbound flights in July 1982.

An aerosol optical model for the July 1982 flight was derived from size distribution measurements made by the University of Wyoming at 27.8°N (Texas) on August 21, 1982 (Hofmann and Rosen, 1983a, 1983b). These measurements provided size distribution data in six size ranges ($r \geqslant 0.01, 0.15, 0.25, 0.95, 1.2$ and 1.8 μm) over an altitude range from 0 to 30 km. With this measured size distribution and assuming sphericity of the particles, Mie calculations were performed at 1 km altitide increments through the stratosphere using index of refraction values represen-

tative of 60-80% solution of sulfuric acid. A model was constructed from these calculations for the conversion of stratospheric integrated backscatter to integrated column density. The conversion value derived that was assumed representative for the July 1982 survey flight was 18.3 g m^{-2} ster.

The integrated backscatter of Figure 8 was divided into bins of 2.5° latitude, and zonal homogeneity was assumed. The conversion of the integrated backscatter yields data on the average column mass density for each latitude bin. These results are shown in Figure 9 for the average of the southbound and northbound data given in Figure 8. Weighting these data by the Earth's surface area for each bin gives the mass loading for the portion of the globe sampled by this flight. The mass values will be discussed subsequently.

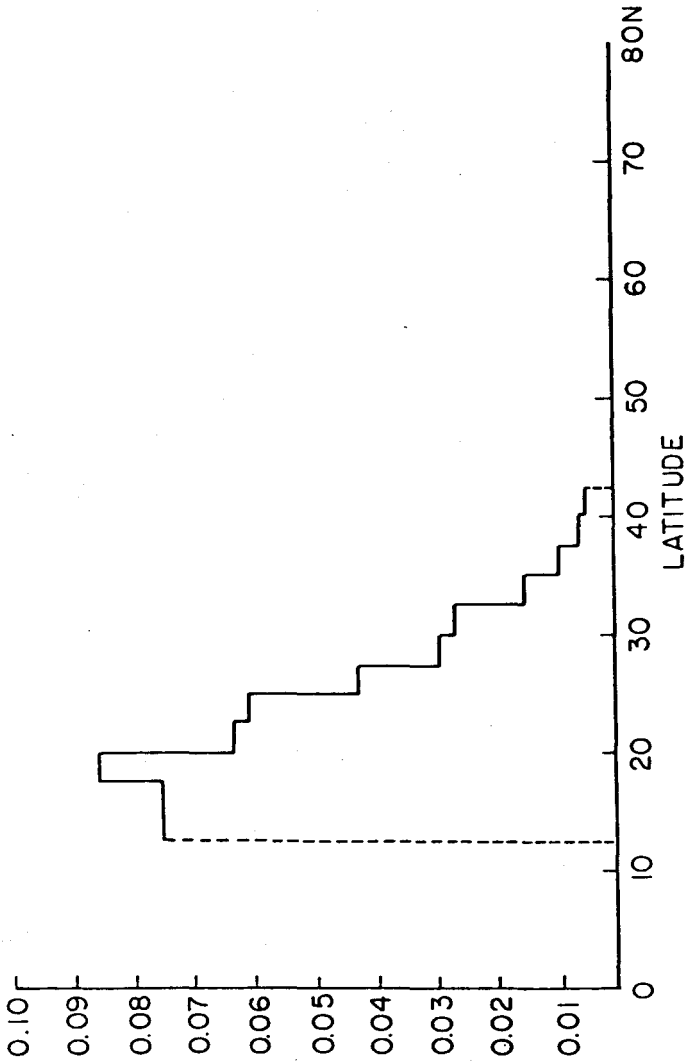

Fig. 9. Column mass density versus latitude for the data of Figure 8 averaged in 2.5° latitude bins. The dashed vertical lines indicate the flight latitude limits.

October-November 1982 campaign

After the July exploratory campaign and with more data becoming available, NASA developed, with the help of the scientific community, a much more ambitious campaign for October/November 1982. The NASA Electra was outfitted with a number of remote and *in situ* sensors, and coordination was made for rendezvous with a number of balloon and aircraft *in situ* measurements over the flight path from the upper central U. S. to southern Chile. Satellite AVHRR and SME coordination was also arranged. Notice of the flight paths and times were circulated to researchers throughout the world so that a larger data set could be brought to bear on this problem. The goal was to determine the key radiative, dynamical, and chemical properties of the El Chichón cloud. In addition, *in situ* sensors were put on board so that a visit to the volcano could be made and sampling of the effluents from the fumaroles accomplished. This part of the emission was coordinated with the Mexican government and was part of the RAVE (Research on Atmospheric Volcanic Emissions) Program (Friend *et al.*, 1982).

Some of the key collaborative measurements to be performed during this campaign were the University of Wyoming dustsonde balloon borne flights in Texas and Wyoming (Hofmann and Rosen, 1983a). The Texas flight utilized their 6-channel size distribution dustsonde with heated inlet so that the additional sulfuric acid mass fraction could be determined.

Figures 10 and 11 present the airborne lidar aerosol backscatter ratio profile data versus latitude for the southbound and northbound legs, respectively, for the October-November 1982 campaign (Flight number 2 on Figure 5). The peak region occurs from about 35°N to 10°S at an altitude of about 23-25 km. Peak backscatter values were about 25, smaller than the July 1982 values of 45. Also, the altitude of the peak was an average of about 1 km lower than the July peak altitude. The integrated aerosol backscatter function for this campaign is given in Figure 12. The most massive and optically thick regions between about 35°N and 10°S are quite evident. Figure 13 averages these data and plots them in 2.5° bins. Figure 14 shows the conversion of these data to mass density using the aerosol properties determined from the dustsonde launch of October 23, 1982, at Del Rio, Texas (29°N) (Hofmann and Rosen, 1983a and 1983b). Calculation of the global mass has been described in McCormick and Swissler (1983) and will be discussed later in the context of all the flights shown in Figure 5. For this survey flight, the conversion value from integrated backscatter to column density was 18.3 g m^{-2} ster. The optical depth data derived from on board sun photometers and lidar data were described by Spinhirne (1983) and Swissler *et al.* (1983), respectively.

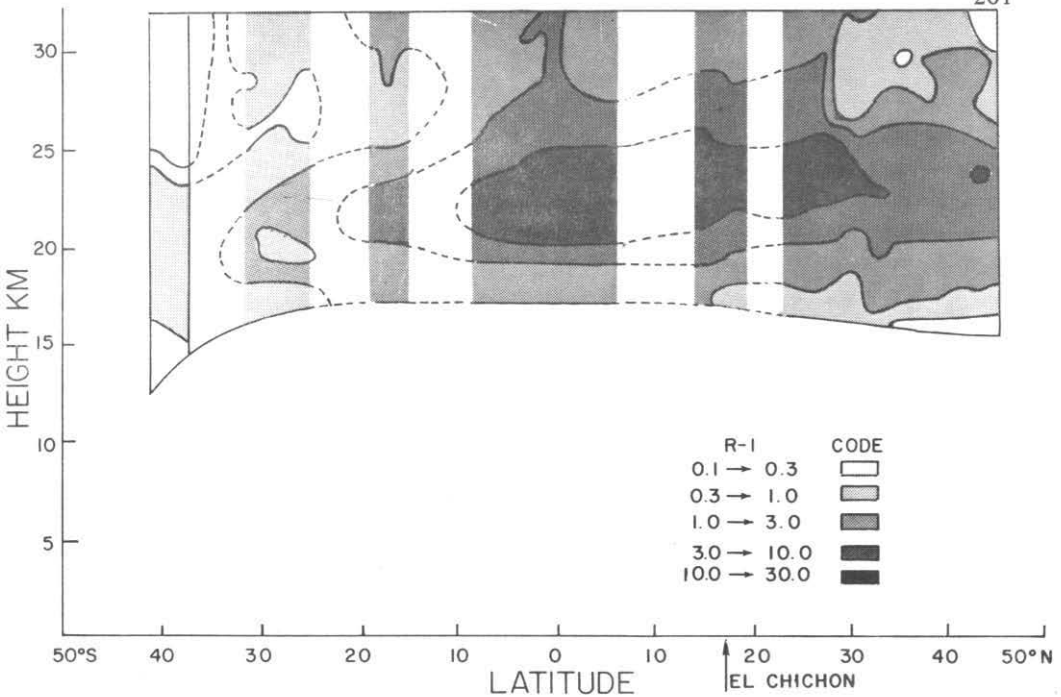

Fig. 10. Contours of aerosol backscatter ratio (R-1) at $\lambda = 0.6943$ μm versus altitude and latitude for the southbound October 19-28, 1982, airborne lidar flight.

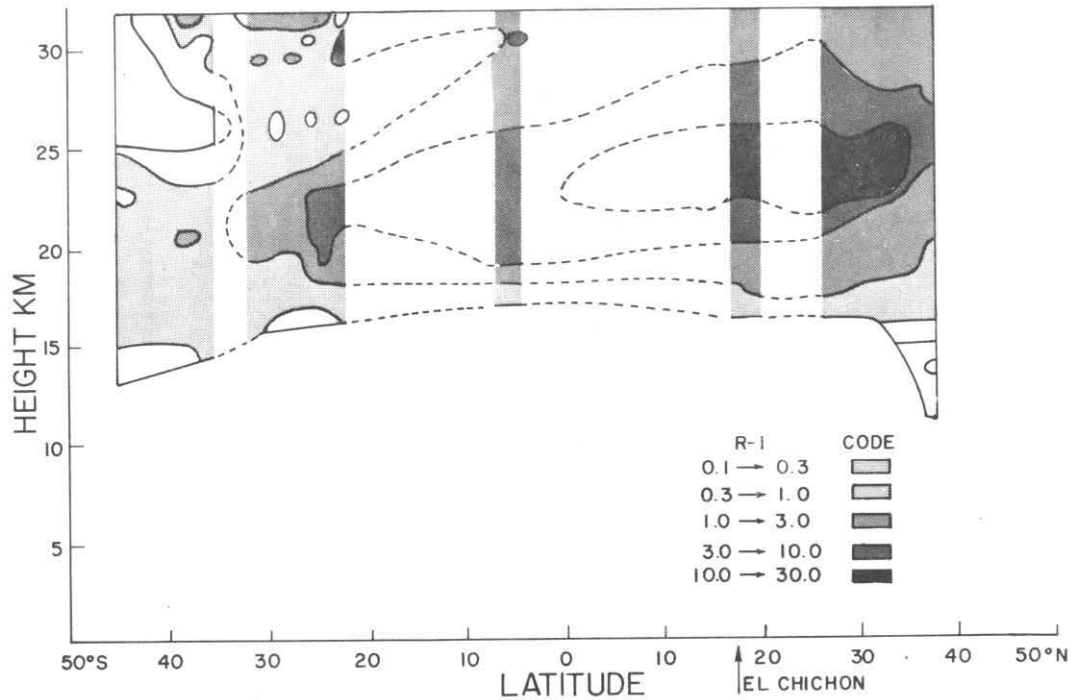

Fig. 11. As in Figure 10 but for the northbound, October 28-November 7, 1982, airborne lidar flight.

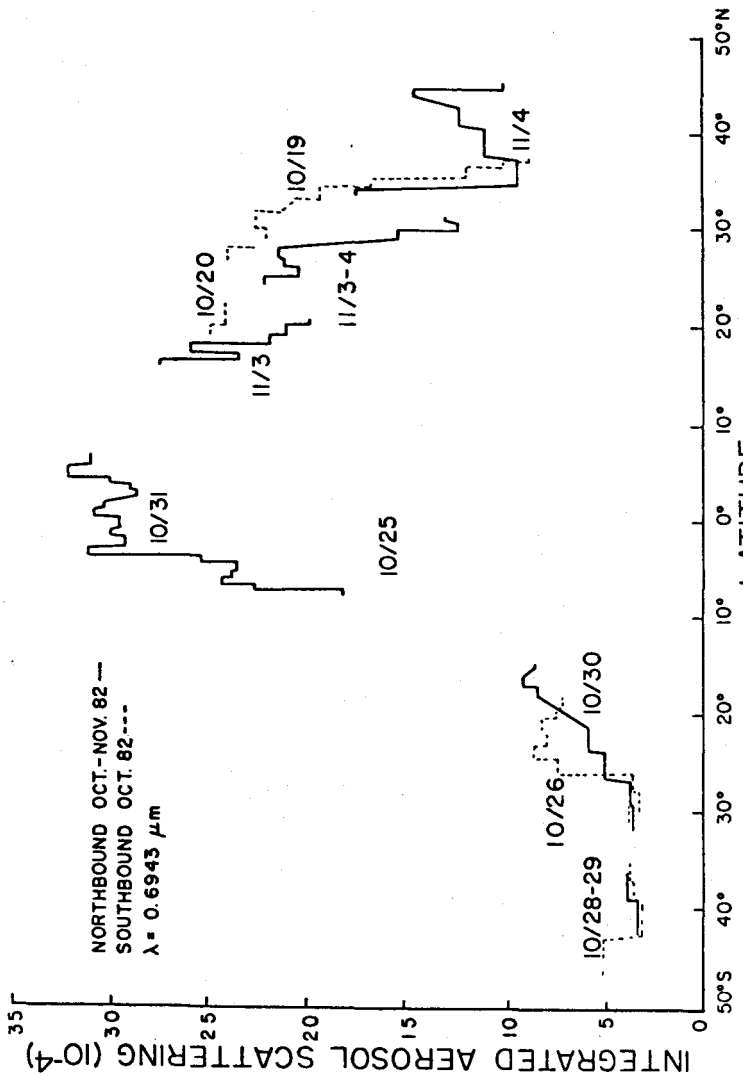

Fig. 12. Integrated aerosol scattering function at $\lambda = 0.6943$ μm for the tropopause through the stratospheric layer versus latitude for the southbound and northbound airborne lidar flights of Figures 10 and 11.

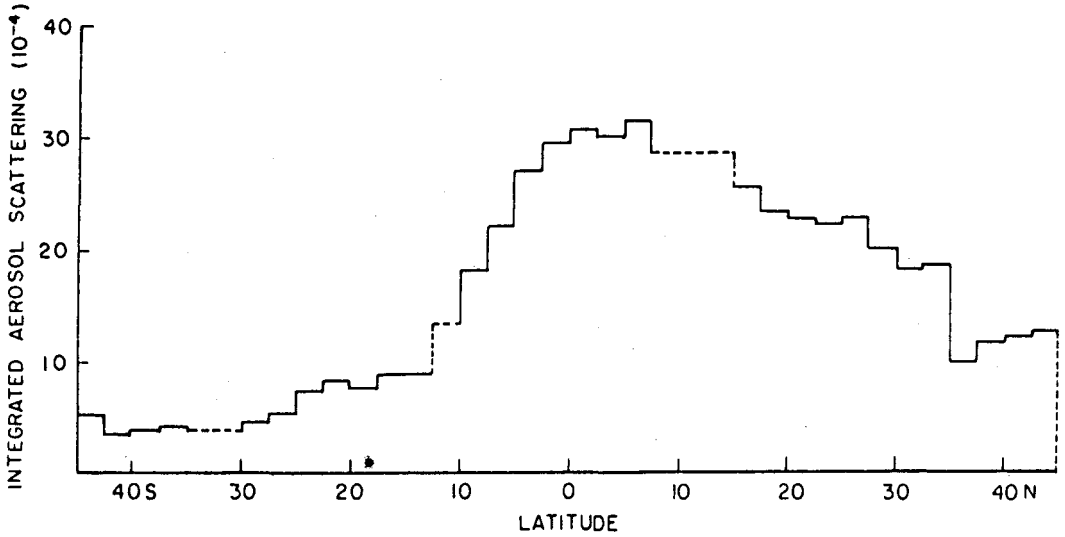

Fig. 13. Integrated scattering function from Figure 12 but averaged into 2.5° latitude bins for both flight legs.

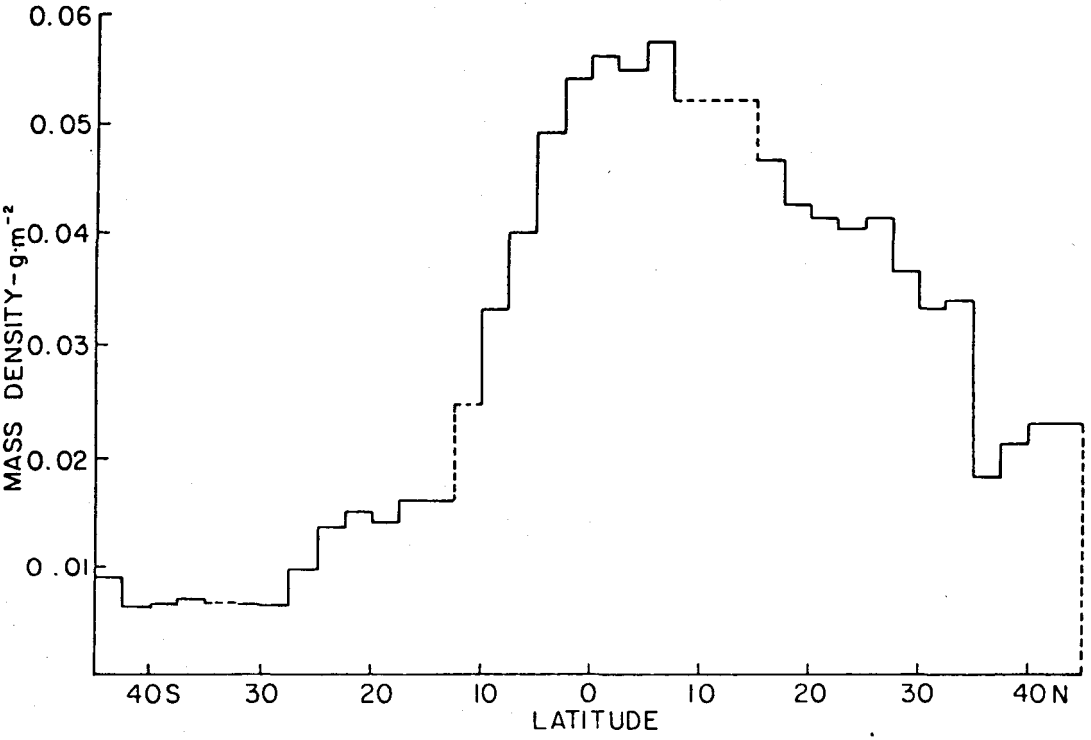

Fig. 14. Column mass density versus latitude for the data in Figure 13. The dashed lines internal to the plot indicate regions where no data were available. The dashed vertical line at 46°N indicates the latitude limit of the flight.

January - February 1983 campaign

The January-February 1983 lidar flight campaign covered latitudes from 27°N to 76°N, from Florida to Greenland and Northern Canada (Flight number 3 on Figure 5). Aerosol ratios versus height and latitude for the northbound and southbound legs of this campaign are shown in Figures 15 and 16, respectively. The peak values varied from about 3 to 10, with the altitude of the peak dropping with higher latitude from about 20 to 15 km. The higher ratios were generally at the lower latitudes. Figure 17 gives the integrated backscatter for each leg, and Figure 18 the average in 2.5° bins.

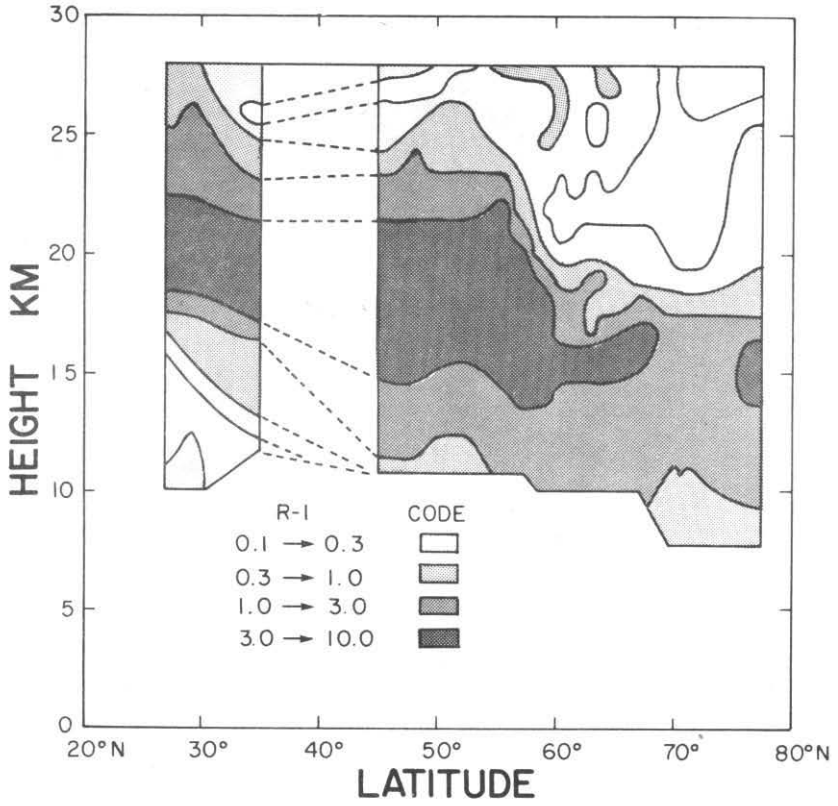

Fig. 15. Contours of aerosol backscatter ratio (R-1) at $\lambda = 0.6943$ μm versus altitude and latitude for the northbound January 27-February 1 and 5, 1983 legs of the airborne lidar campaign.

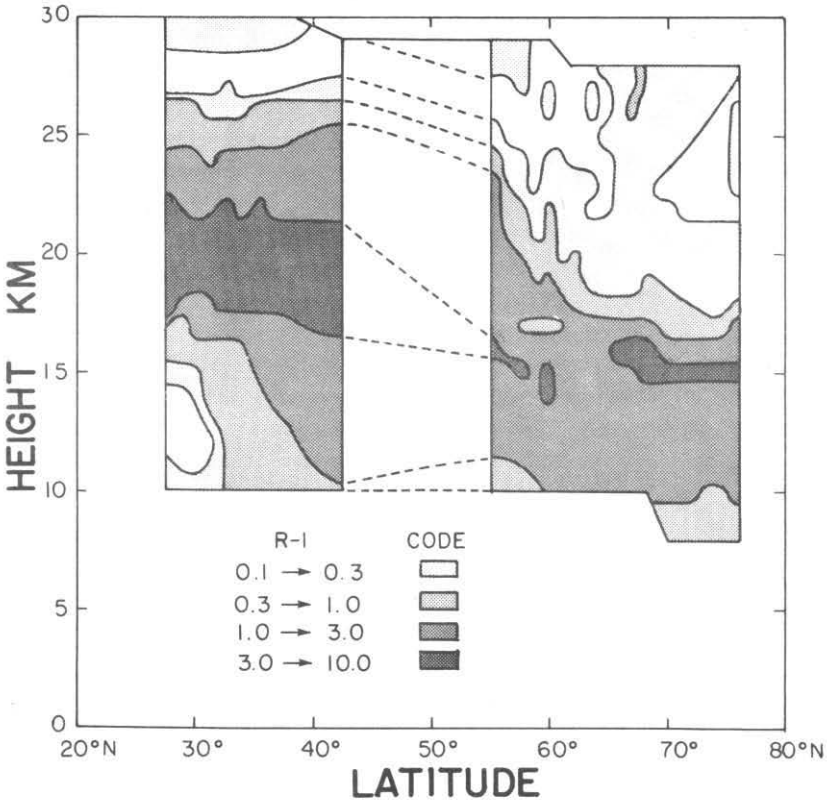

Fig. 16. Same as in Figure 15 but for the southbound leg February 2-4, 1983.

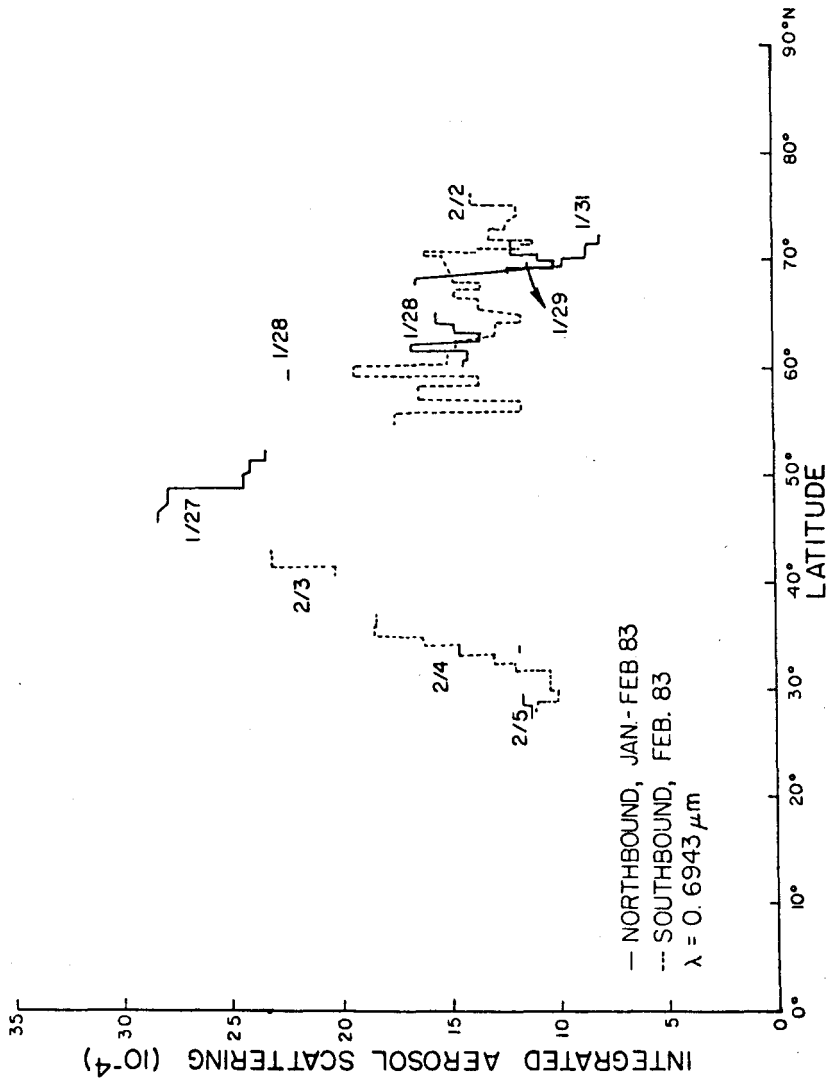

Fig. 17. Integrated aerosol scattering function for the data of Figures 15 and 16 calculated from the tropopause through the stratospheric layer.

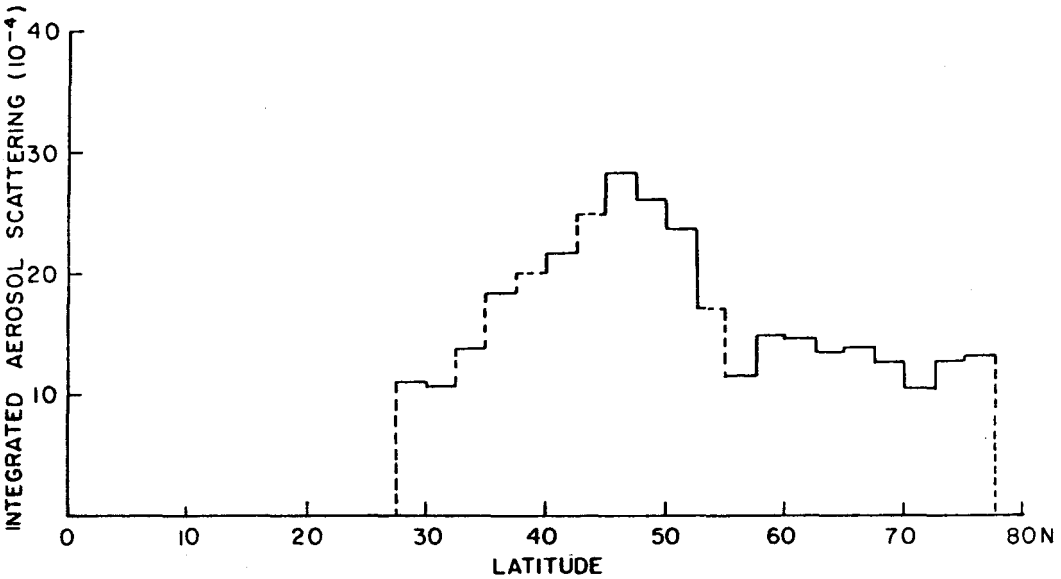

Fig. 18. The data of Figure 17 averaged into 2.5° latitude bins.

Figure 19 shows the results for the integrated column density using a conversion value from integrated backscatter derived from the 6-channel dustsonde launch of January 28, 1983, at Laramie, Wyoming (41°N). As before, an aerosol optical model was constructed with the measured size distribution data. A value of 20.5 g m^{-2} ster was used to convert these data to mass density. Note that the peak in mass density occurs near 45°N with a peak value not too much different than the peak values at 0-10°N found during the October-November 1982 flight campaign.

Shown in Figure 20 are representative profiles near 28°N latitude taken with the airborne lidar during the July 1982, October 1982, and February 1983 surveys. Note the decrease in time of the peak backscatter ratio, both in magnitude and in altitude. Also evident is the spreading in the width of the layer as it ages.

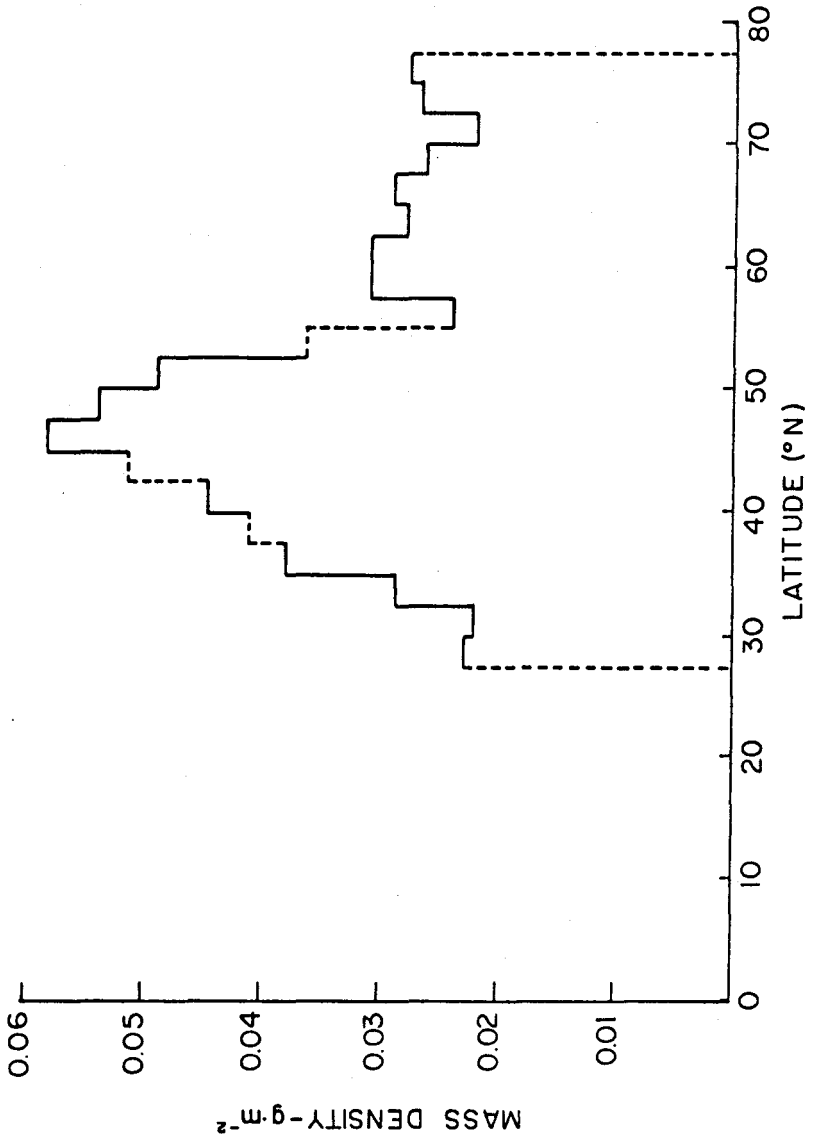

Fig. 19. Column mass density for the data in Figure 18.

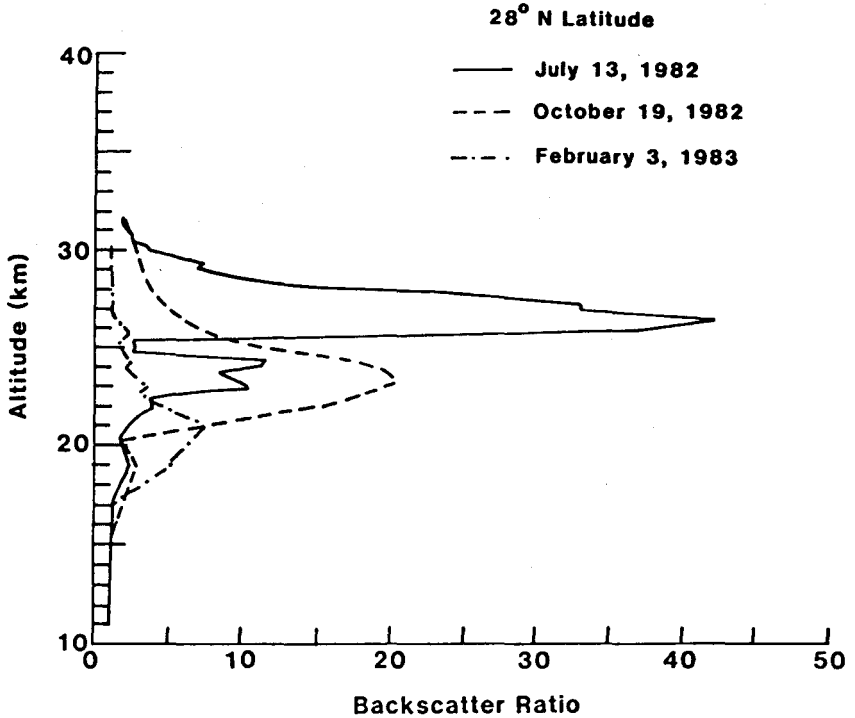

Fig. 20. Lidar profiles of backscatter ratio (R) at $\lambda = 0.6943$ μm versus altitude for airborne measurements taken at 28°N.

May 1983 campaign

The May 1983 mission over the Pacific (Flight number 4 in Figure 5) covered latitudes from 72°N to 56°S. The southbound leg backscatter ratio data are shown in Figure 21 (May 11-17, 1983), and Figure 22 is for the northbound leg (May 9, May 17-21, 1983). The first flight segment was from California to Alaska on May 9, 1983. Peak lidar backscatter ratio values varied between 3.8 at 18.3 km and 41°N, 4 at 16.4 km and 58°N, and 3.7 at 14.4 km at 70°N. Examples of values for other segments are: near 30°N, values of 6 at 20 km were recorded; at 16°N, 7 at 21 km; at 8°N, 8.4 at 22 km; at 20°S, 4.4 at 20.4 km; at 23°S, 3.6 at 22 km; at 30°S, 3 at 19.4 km; dropping below 3 all the way to 41°S in New Zealand. The values south of New Zealand were similar, but the error bars were high due to sunlight conditions and thus uncertain normalization. This lidar normalization problem is reflected in the error bars of Figure 23 which plots the average integrated aerosol backscatter versus latitude. The largest error bars shown at high latitudes, however, are due to the high altitude of flight experienced on these segments. That is, the lidar profiles do not include the entire layer since the layer is lower at high latitudes

(reflecting the lower tropopause), and the aircraft, therefore, was flying in the layer. An estimate was made for integrated aerosol backscatter from the tropopause up to the aircraft altitude based on aircraft lidar measurements made at lower latitudes.

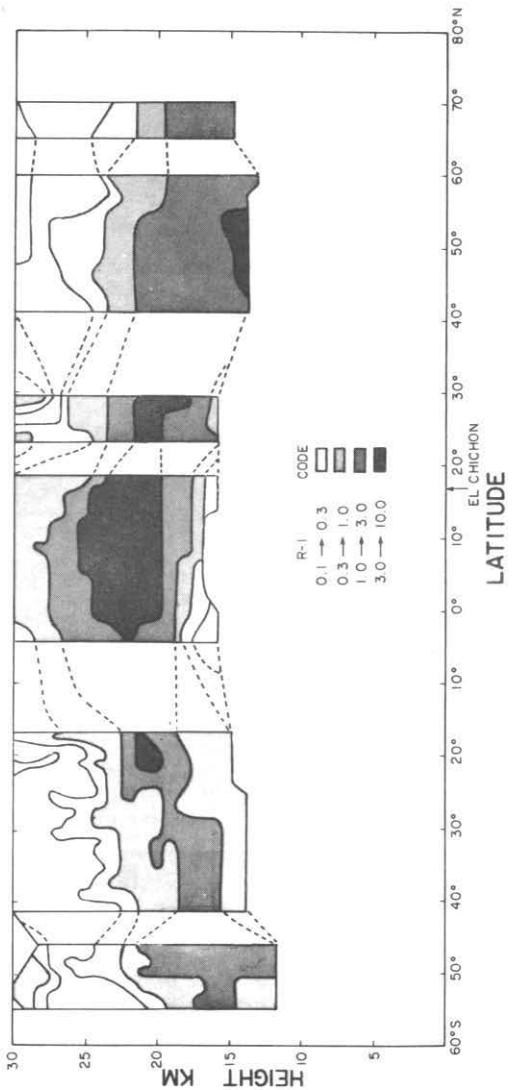

Fig. 21. Contours of aerosol backscatter ratio (R-1) at $\lambda = 0.6943$ μm versus altitude and latitude for the southbound flight leg May 11-17, 1983.

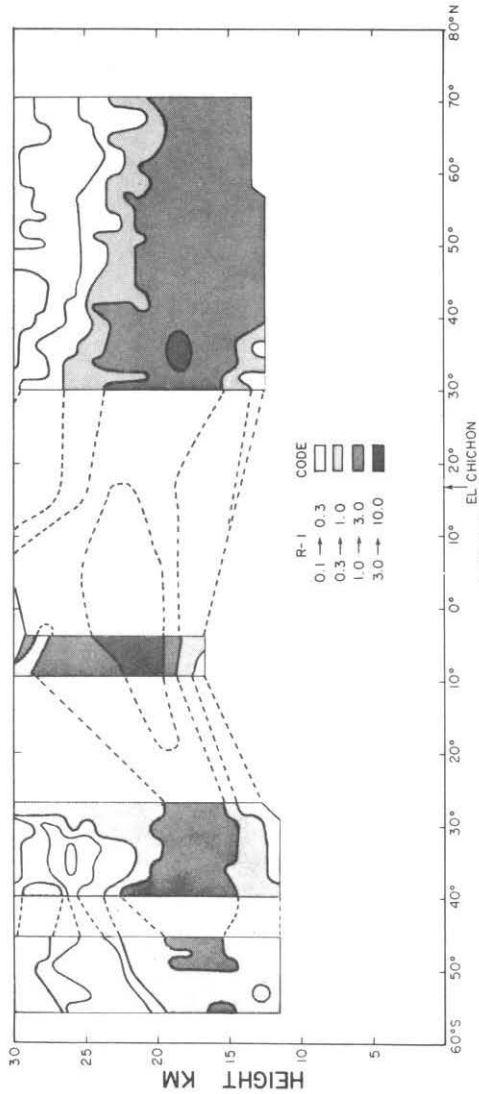

Fig. 22. Same as Figure 21 but for the northbound flight legs of May 9 and May 17-21, 1983.

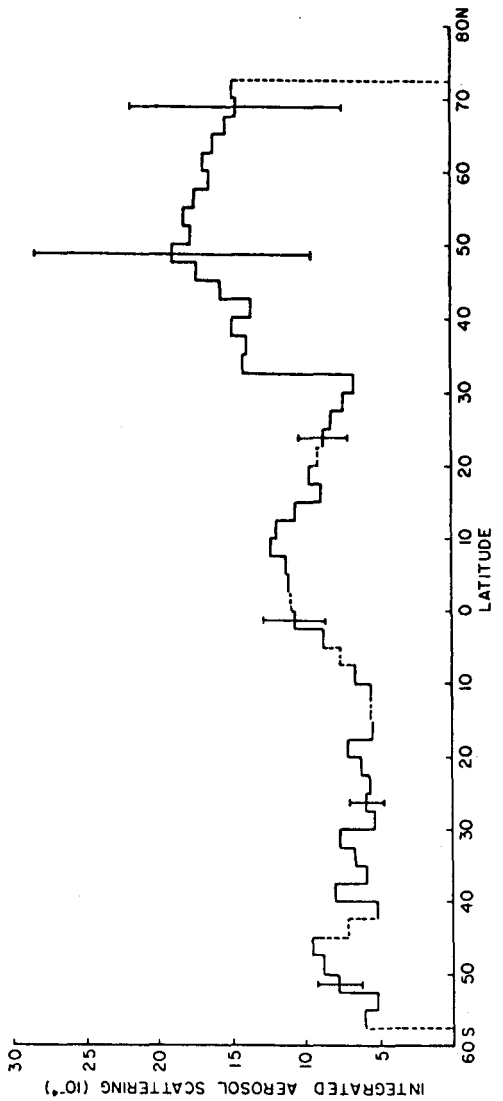

Fig. 23. Integrated aerosol scattering function averaged in 2.5° latitude bins for the data of Figures 21 and 22. Vertical error bars show the uncertainty in this calculation.

As can be seen in Figure 23, the material appears well spread throughout the latitudes of 56°S to 72°N. Local peaks appear to be near 10°N, 50°N, and possibly 45°S with minima near 30°N and possibly 10 to 30°S (but not as well defined). The largest peak appears near 50°N, not too much different in position than what it was in January 1983, but lower in magnitude. The mass density plot is given in Figure 24. For this survey the value used for converting the integrated backscatter to column density was 21.6 g m^{-2} ster based on a six-channel dustsonde flight from Palestine, Texas (32°N) on May 16, 1983.

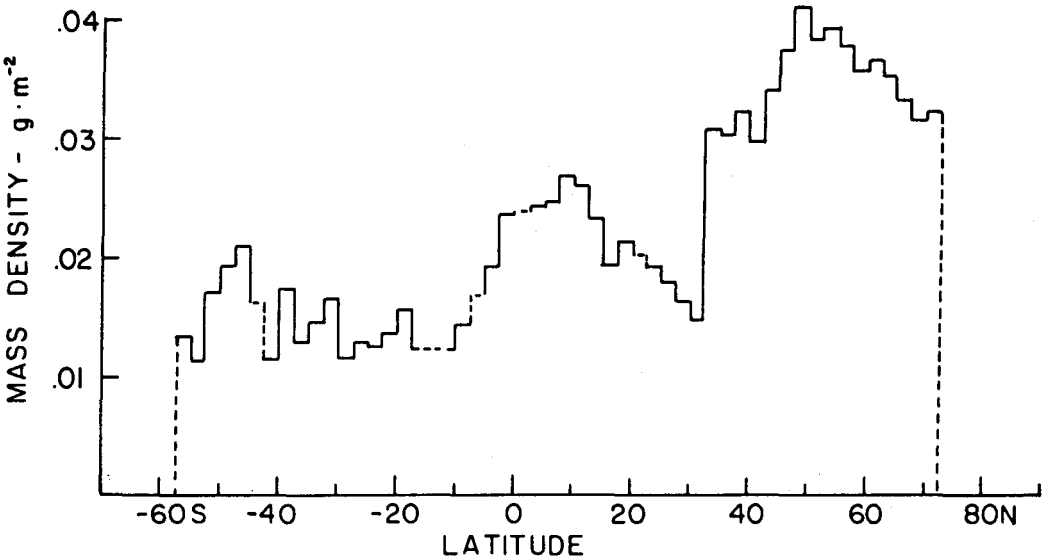

Fig. 24. Column mass density for the data in Figure 23.

January 1984 campaign

The most recent flight campaign was flown in late January 1984, from Virginia (37°N) to the North Pole. Note that this occurred after the IUGG meeting, but was added here for completeness. The flight track was through Goose Bay, Canada, and Greenland with the flight from Thule to the Pole along the 60°W longitude. Typical values of peak backscatter ratio were from 2.3 at 16 km at 42°N, to 3.0 at 13.4 km at 68°N. Polar stratospheric clouds (McCormick *et al.*, 1982) contaminated the profiles above 15 km north of Thule (76°N). The mass density plot for this trip has been constructed utilizing a conversion value derived from a dustsonde launch on December 21, 1983, from Laramie, Wyoming. As previously, an optical aerosol model was constructed with this dustsonde data. A conversion value of 21.3 g m^{-2} was derived for this survey. The results are shown in Figure 25 with the lidar data averaged into 2.5° latitude bins.

MASS LOADINGS

In order to calculate the mass associated with the airborne lidar measurements, an aerosol optical model was constructed from the aerosol size distribution measurements (Hofmann and Rosen, 1983a, 1983b). The dustsonde measurements utilized were those closest in time and location for each of the survey flights. As shown previously, the integrated aerosol backscatter for these flights was divided into bins of 2.5° latitude, and zonal homogeneity was assumed. The conversion values employed for each trip have been described above and the results plotted in Figure 9 for the July 1982 flight; Figure 14 for the October-November 1982 flight; Figure 19 for the January-February 1983 flight; Figure 24 for the May 1983 flight; and Figure 25 for January 1984 flight. The data for these plots are given in Table 2-A for the Northern Hemisphere and in Table 2-B for the Southern Hemisphere. The

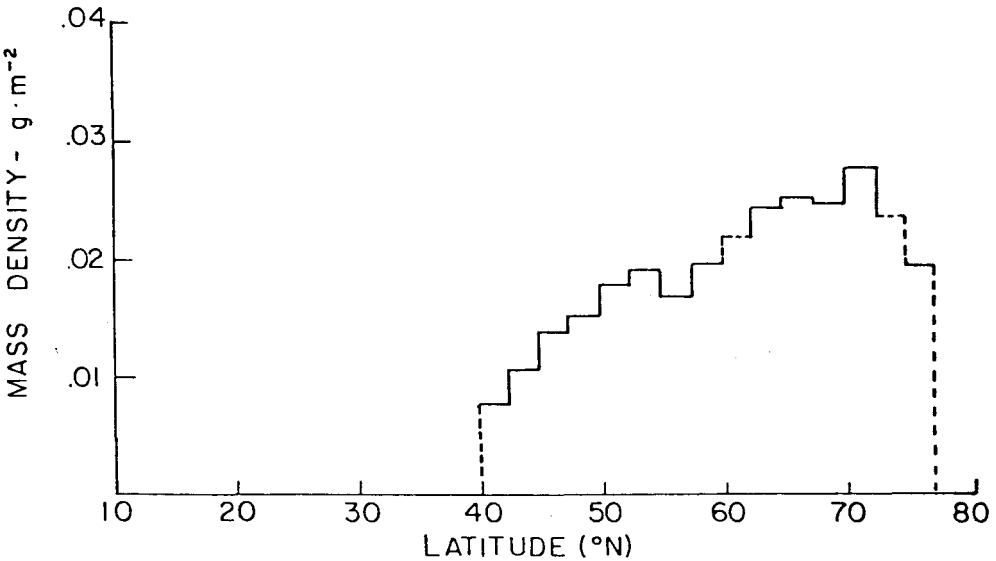

Fig. 25. Column mass density versus latitude for the survey flight of January 1984. Data have been averaged into 2.5° latitude bins.

column mass densities for each of the flights are given so that the time evolution (including decay) at various latitudes can be determined. Weighting these data by the earth's surface area for each bin yields the stratospheric mass loading for that latitude range. The results are listed in Table 3 with the fraction of the earth's surface given for each latitude range. The total mass for each survey (that is, for the latitudes covered on each survey) is given at the bottom of the table. A total global mass value of 12 megatonnes, for example, was found for the October-November Campaign by extrapolating the mass density values to higher latitudes and substracting off the pre-El Chichón global background derived by SAGE measurements (McCormick and Swissler, 1983).

Table 2 A

El Chichón survey flights

Col. density ($x10^{-2}$ g m^{-2}) per latitude band

Northern hemisphere

Latitude band	July 82	Oct/Nov 82	Jan/Feb 83	May 83	Jan 84
77.5 - 75.0°N			2.71		1.92
75.0 - 72.5			2.62		2.34*
72.5 - 70.0			2.16	3.20	2.76
70.0 - 67.5			2.59	3.14	2.46
67.5 - 65.0			2.87	3.30	2.50
65.0 - 62.5			2.77	3.49	2.41
62.5 - 60.0			3.03	3.64	2.17*
60.0 - 57.5			3.05	3.54	1.92
57.5 - 55.0			2.37	3.76	1.67
55.0 - 52.5			3.60*	3.92	1.89
52.5 - 50.0			4.84	3.82	1.78
50.0 - 47.5			5.32	4.08	1.50
47.5 - 45.0			5.78	3.73	1.37
45.0 - 42.5		2.29	5.09*	3.39	1.07
42.5 - 40.0	0.58	2.29	4.41	2.93	0.74
40.0 - 37.5	0.67	2.15	4.08*	3.21	
37.5 - 35.0	0.98	1.82	3.76	2.99	
35.0 - 32.5	1.54	3.38	2.83	3.05	
32.5 - 30.0	2.69	3.32	2.19	1.44	
30.0 - 27.5	2.89	3.64	2.24	1.60	
27.5 - 25.0	4.23	4.14		1.76	
25.0 - 22.5	6.04	4.03		1.88	
22.5 - 20.0	6.30	4.12		1.99*	
20.0 - 17.5	8.55	4.24		2.10	
17.5 - 15.0	7.48	4.65		1.90	
15.0 - 12.5	7.47	4.91*		2.30	
12.5 - 10.0		5.17*		2.57	
10.0 - 7.5		5.43*		2.65	
7.5 - 5.0		5.70		2.43	
5.0 - 2.5		5.44		2.40	
2.5 - 0		5.57		2.36*	

* interpolated data

Table 2 B

El Chichón survey flights
Col. density ($x10^{-2}$ g m^{-2}) per latitude band

Southern hemisphere

Latitude band	July 82	Oct/Nov 82	Jan/Feb 83	May 83	Jan 84
0.0 - 2.5°S		5.37		2.32	
2.5 - 5.0		4.90		1.89	
5.0 - 7.5		4.03		1.65*	
7.5 - 10.0		3.30		1.41	
10.0 - 12.5		2.45*		1.19	
12.5 - 15.0		1.60		1.18*	
15.0 - 17.5		1.60		1.17	
17.5 - 20.0		1.39		1.53	
20.0 - 22.5		1.49		1.33	
22.5 - 25.0		1.36		1.22	
25.0 - 27.5		0.96		1.25	
27.5 - 30.0		0.63		1.12	
30.0 - 32.5		0.67		1.63	
32.5 - 35.0		0.68*		1.42	
35.0 - 37.5		0.70		1.25	
37.5 - 40.0		0.65		1.71	
40.0 - 42.5		0.62		1.12	
42.5 - 45.0		0.93		1.59*	
45.0 - 47.5				2.06	
47.5 - 50.0				1.89	
50.0 - 52.5				1.67	
52.5 - 55.0				1.10	
55.0 - 57.5				1.31	

* interpolated data

Table 3 A

El Chichón survey flights

Stratospheric mass (megatonnes) per latitude band

Northern hemisphere

Latitude band	July 82	Oct/Nov 82	Jan/Feb 83	May 83	Jan 84	% Earth's Surface
77.5 - 75.0°N			0.07		0.05	0.5
75.0 - 72.5			0.08		0.07*	0.6
72.5 - 70.0			0.08	0.11	0.10	0.7
70.0 - 67.5			0.10	0.13	0.10	0.8
67.5 - 65.0			0.13	0.15	0.11	0.9
65.0 - 62.5			0.14	0.17	0.12	1.0
62.5 - 60.0			0.16	0.20	0.11*	1.0
60.0 - 57.5			0.18	0.20	0.11	1.1
57.5 - 55.0			0.14	0.23	0.10	1.2
55.0 - 52.5			0.24*	0.26	0.13	1.3
52.5 - 50.0			0.34	0.27	0.12	1.4
50.0 - 47.5			0.39	0.30	0.11	1.4
47.5 - 45.0			0.45	0.29	0.11	1.5
45.0 - 42.5		0.18	0.41*	0.27	0.09	1.6
42.5 - 40.0	0.05	0.19	0.37	0.25	0.06	1.6
40.0 - 37.5	0.06	0.19	0.35*	0.28		1.7
37.5 - 35.0	0.09	0.16	0.34	0.27		1.8
35.0 - 32.5	0.14	0.31	0.26	0.28		1.8
32.5 - 30.0	0.26	0.32	0.21	0.14		1.9
30.0 - 27.5	0.28	0.36	0.22	0.16		1.9
27.5 - 25.0	0.42	0.41		0.18		2.0
25.0 - 22.5	0.62	0.41		0.19		2.0
22.5 - 20.0	0.65	0.43		0.21*		2.0
20.0 - 17.5	0.90	0.45		0.22		2.1
17.5 - 15.0	0.80	0.50		0.20		2.1
15.0 - 12.5	0.81	0.53*		0.25		2.1
12.5 - 10.0		0.57*		0.28		2.1
10.0 - 7.5		0.60*		0.29		2.2
7.5 - 5.0		0.63		0.27		2.2
5.0 - 2.5		0.60		0.27		2.2
2.5 - 0		0.62		0.26*		2.2
Subtotal	5.08	7.46	4.66	6.58	1.49	

* interpolated data

Table 3 B

El Chichón survey flights

Stratospheric mass (megatonnes) per latitude band

Southern hemisphere

Latitude band	July 82	Oct/Nov 82	Jan/Feb 83	May 83	Jan 84	% Earth's Surface
0.0 - 2.5		0.60		0.26		2.2
2.5 - 5.0		0.55		0.21		2.2
5.0 - 7.5		0.45		0.18*		2.2
7.5 - 10.0		0.36		0.15		2.2
10.0 - 12.5		0.27*		0.13		2.1
12.5 - 15.0		0.18		0.13		2.1
15.0 - 17.5		0.17		0.13		2.1
17.5 - 20.0		0.15		0.16		2.1
20.0 - 22.5		0.15		0.14		2.0
22.5 - 25.0		0.14		0.12		2.0
25.0 - 27.5		0.10		0.12		2.0
27.5 - 30.0		0.06		0.11		1.9
30.0 - 32.5		0.06		0.16		1.9
32.5 - 35.0		0.06		0.13		1.8
35.0 - 37.5		0.06		0.11		1.8
37.5 - 40.0		0.06		0.15		1.7
40.0 - 42.5		0.05		0.09		1.6
42.5 - 45.0		0.07		0.13		1.6
45.0 - 47.5				0.16		1.5
47.5 - 50.0				0.14		1.4
50.0 - 52.5				0.12		1.4
52.5 - 55.0				0.07		1.3
55.0 - 57.5				0.08		1.2
Subtotals		3.54		3.18		
Totals	5.08	11.00	4.66	9.76	1.49	

* interpolated data

The global mass estimated from all these surveys seems to have peaked probably in the time interval between the July and October-November 1982 mission. These airborne surveys have yielded important new information about the distribution and transport of the El Chichón volcanic cloud. However, a complete picture of the global impact can only come from continuous global sampling of the stratosphere such as available from satellite measurements combined with measurements of the various aerosol physical and optical properties at specific locations as a function of time.

SUMMARY

This paper has presented lidar data taken by NASA in a number of airborne campaigns designed to study effects of the El Chichón eruption on the stratosphere, remote sensors, and the earth's radiation budget. Also, ground-based lidar data were described putting this eruption into a historical perspective with other volcanic impacts to the stratosphere at 37°N over the past 10 years. The ground-based data show the El Chichón enhancement to be the largest by far that has occurred in the last 10 years, and based on other data, probably the largest enhancement to the Northern Hemisphere that has occurred in the last 70 years. The trend at 37°N since 1980 has been an increase in stratospheric loading with a peak value in January 1983, 100 times that in 1979. During the same period the peak areosol backscatter ratio increased by as much as a factor of 400 to 600. Lidar profiles taken after the peak in aerosol ratio and integrated amount showed the characteristic lowering in peak value and broadening in width of the layer.

The airborne campaigns covered the latitudes 90°N to 56°S over the period July 1982 to January 1984. Extensive coordination with *in situ* and other remote measurements was accomplished. The early flights showed the most massive and optically thick stratospheric material to be above 20 km and was constrained between about 30°N to 10°S for the first 6 months. The extremes of these latitude limits appeared to be variable from day to day depending on synoptic meteorology. The lower material below about 20 km moved toward higher latitudes much more rapidly; the Langley lidar observed this material to reach 37°N as early as April 29, 1982. The first significant layer above 20 km was observed on June 2 and the largest on July 1 with a backscatter ratio of about 45. These upper altitude observations, however, were transient and due to pieces of the main low latitude belt of material being transported overhead. The bulk of this material remained at low northern latitudes.

A global mass calculation was performed based on the data from the fall 1982 campaign and associated supporting measurements. The value derived was 12 megatonnes (1.2×10^{13} g) for the total globe at this time after substracting out the preexisting loading.

The subsequent campaigns in the winters of 1983 and 1984 and in the late spring of 1983 showed the material spreading globally and mixing downward in altitude. The peak scattering ratios and column mass values decreased once peaked at a given latitude. The layer at 28°N in July 1982, for example, peaked at 27 km but by February 1983 the peak moved downward to 21 km. In May 1983, the peak backscatter ratios at 55°N and 55°S were at about 16-17 km. In the polar regions the peaks in winter 1984 were at about 13-14 km. The integrated aerosol scattering function or column mass density appeared to peak at approximately 50°N by the

late spring of 1983 and 70° in the winter of 1984. The column mass densities for each of the flights are given so that the time evolution (including decay) at various latitudes can be determined. The global mass maximum is thought to have peaked prior to the fall of 1982. As with other stratospheric constituents, the altitudes of the peak backscatter ratios were lower with higher latitude.

The data obtained from these surveys present a unique set of measurements for climate models and for an assessment of the impact of the El Chichón stratospheric cloud on the earth's radiation budget and remote sensors. Further analysis of the global impact of these aerosols and a description of the decay of the stratospheric mass loading will be the subject of future contributions.

ACKNOWLEDGEMENTS

The authors recognize the untiring efforts of B. R. Rouse and F. C. Diehl in supporting the lidar measurements, and wish to thank the crews and supporting personnel at NASA Wallops Flight Center (Electra) and the Ames Research Center (CV-990) for providing excellent research aircraft platforms for conducting these measurements. In addition, thanks go out to the many groups at the various U. S. Air Force Bases, and the Governments of Mexico, Greenland, Peru, Chile, Samoa, Canada, and New Zealand, that provided logistics support during the missions. Finally, the authors wish to express their appreciation to D. J. Hofmann and J. M. Rosen of the University of Wyoming for providing the dustsonde data for each of the flight campaigns.

BIBLIOGRAPHY

BARTH, C. A., R. W. SANDERS, R. J. THOMAS, G. E. THOMAS, B. M. JAKOSKY, and R. A. WEST, 1983. Formation of the El Chichón aerosol cloud. *Geophys. Res. Lett., 10,* 993-996.

FRIEND, J. P., A. R. BANDY, J. L. MOYERS, W. H. ZOLLER, R. E. STOIBER, A. L. TORRES, W. I. ROSE, M. P. McCORMICK, and D. C. WOODS, 1982. Research on atmospheric volcanic emissions: An overview. *Geophys. Res. Lett., 9,* 1101-1104.

HOFMANN, D. J. and J. M. ROSEN, 1983a. Stratospheric sulfuric acid fraction and mass estimate for the 1982 volcanic eruption of El Chichón. *Geophys. Res. Lett., 10,* 313-316.

HOFMANN, D. J. and J. M. ROSEN, 1983b. Sulfuric acid droplet formation and growth in the stratosphere after the 1982 eruption of El Chichón. *Science, 223,* 325-327.

LABITZKE, K., B. NAUJOKAT, and M. P. McCORMICK, 1983. Temperature effects on the stratosphere of the April 4, 1982 eruption of El Chichón, Mexico. *Geophys. Res. Lett., 10,* 24-26.

LABITZKE, K. and B. NAUJOKAT, 1984. On the effect of the volcanic eruptions of Mount Agung and El Chichón on the temperature of the stratosphere. *Geof. Int.*, this issue.

MATSON, M. and A. ROBOCK, 1984. Satellite detection of the 1982 El Chichón eruptions and stratospheric dust cloud. *Geof. Int.*, this issue.

McCORMICK, M. P., P. HAMILL, T. J. PEPIN, W. P. CHU, T. J. SWISSLER, and L. R. McMASTER, 1979. Satellite studies of the stratospheric aerosol. *Bull. Amer. Meteor. Soc., 60,* 1038-1046.

McCORMICK, M. P., H. M. STEELE, P. HAMILL, W. P. CHU, and T. J. SWISSLER, 1982. Polar stratospheric cloud sightings by SAM II. *J. Atmos. Sci., 39,* 1387-1397.

McCORMICK, M. P., 1983. Aerosol measurements from earth orbiting spacecraft. *Adv. Space Res., 2,* 73-86.

McCORMICK, M. P. and T. J. SWISSLER, 1983. Stratospheric aerosol mass and latitudinal distribution of the El Chichón eruption cloud for October 1982. *Geophys. Res. Lett., 10,* 877-880.

McCRACKEN, M. C. and F. M. LUTHER, 1984. Preliminary estimate of the radiative and climatic effects of the El Chichón eruption. *Geof. Int.*, this issue.

NEWELL, R. E. and A. DEEPAK, 1982. Mount St. Helens eruptions of 1980. Atmospheric effects and potential climatic impact. NASA SP *458.*

POLLACK, J. B. and J. P. ACKERMAN, 1983. Possible effects of the El Chichón volcanic cloud on the radiation budget of the Northern Tropics. *Geophys. Res. Lett., 10,* 1057-1060.

QUIROZ, R. S., 1983. Influence of the El Chichón eruption on the stratosphere after summer 1982. *Geof. Int.*, this issue.

ROBOCK, A., 1984. Climate model simulations of the effects of the El Chichón eruption. *Geof. Int.*, this issue.

SPINHIRNE, J. D., 1983. El Chichón eruption cloud: Latitudinal variation of spectral optical thickness for October 1982. *Geophys. Res. Lett., 10,* 881-884.

STRONG, A. E., 1984. Monitoring El Chichón aerosol distribution using NOAA-7 satellite AVHRR sea surface temperature observations. *Geof. Int.*, this issue.

SWISSLER, T. J., M. P. McCORMICK, J. D. SPINHIRNE, 1983. El Chichón eruption cloud: Comparison of lidar and optical thickness measurements for October 1982. *Geophys. Res. Lett., 10,* 885-888.

VUPPUTURI, R. K R. and J. P. BLANCHET, 1984. The possible effects of El Chichón eruption on atmospheric thermal and chemical structure and surface climate. *Geof. Int.*, this issue.

(Accepted: February 20, 1984)